Thermochimica Acta 724 (2023) 179491

Contents lists available at ScienceDirect

Thermochimica Acta

journal homepage: www.elsevier.com/locate/tca

A study of thermal etching of GaN by atmospheric argon inductively coupled plasma

Linfeng Zhang [a], Yongjie Zhang [a,b], Bing Wu [a], Hui Deng [a,*]

[a] Department of Mechanical and Energy Engineering, Southern University of Science and Technology, No. 1088, Xueyuan Road, Shenzhen, Guangdong 518055, China
[b] Department of Physics and Centre for Advanced 2D Materials, National University of Singapore, 2 Science Drive 3, Singapore 117551, Singapore

ARTICLE INFO

Keywords:
Thermal etching
GaN
Inductively coupled plasma
Damage relief

ABSTRACT

GaN has a wide application in electronics and optoelectronics due to its excellent electrical properties. The thermal etching process is commonly used in the growth and subsequent process of GaN. As an easy-to-operate technique, atmospheric argon inductively coupled plasma (Ar-ICP) is first applied to the thermal etching of GaN in this study. Through the analysis of surface chemical composition and near-surface plasma spectroscopy, the etching principle and mechanism of the circular etching pit formation are revealed. The maximum material removal rate of Ar-ICP thermal etching can reach 18.72 μm/min. The optical properties of the sliced GaN after the Ar-ICP thermal etching and lapping process are evaluated by photoluminescence (PL), respectively. The PL intensity of the Ar-ICP thermally etched sample increases and the peak position of near-band emission shows a red shift compared to the lapped sample.

1. Introduction

GaN is a promising material with many excellent properties and has been widely used in electronic and optoelectronic devices [1–3]. The thermal etching process is commonly used in the growth and subsequent process of GaN, such as the intermediate step to modulate the growth conditions and the post-annealing for the relief of the stress state. The current researches mainly study the thermal etching of GaN from the perspective of regulating crystal growth. For example, Song et al. have developed an in-situ thermal etching process as the intermediate step in the crystal growth process to form etch facets [4]. Lateral growth is then performed from these facets and achieves the improvement of crystal and optical qualities. Koblmüller et al. have employed N-rich conditions at temperatures of GaN thermal decomposition and achieved dislocation reduction in AlGaN/GaN hetero-structures [5]. In addition, GaN nano-hole arrays with high aspect ratios have been prepared by selective area thermal etching without introducing ion damage [6]. Many studies have confirmed the thermal decomposition phenomenon and mechanism of GaN at high temperatures. Several possible reactions have been proposed as follows: decomposition of GaN into gaseous gallium, nitrogen atoms, and nitrogen; the decomposition of GaN into Ga and nitrogen; the sublimation of GaN [7–10]. However, the mechanism of thermal etching of GaN needs further verification. We first utilize an atmospheric argon inductively coupled plasma (Ar-ICP) torch as the heat source to realize the thermal etching of GaN. The characteristics of Ar-ICP thermal etching GaN and its damage relief effect are investigated. The Ar-ICP thermal etching is easy to operate under the atmosphere, which eliminates the requirement for expensive high vacuum maintenance systems and time-consuming vacuuming processes.

In this study, we demonstrate the etching principle and surface evolution mechanism during the Ar-ICP thermal etching. It is also revealed that the Ar-ICP thermal etching has a higher material removal rate than the lapping process, and can achieve damage relief rather than induce new damage.

2. Experimental methods

Unintentionally-doped freestanding GaN wafers supplied by Suzhou Nanowin Co. Ltd. were used in this work. The size of the sample is 10 × 10 mm, with a thickness of 350 ± 25 μm. The dislocation density of the sample is 1×10^{-6} cm^{-2}. The initial surface has a roughness of around *Sa* 0.5 nm. Before and after thermal etching, the samples were ultrasonically cleaned with absolute ethyl alcohol for 10 min to remove the contaminants, followed by rinsed with deionized water to remove residual alcohol.

Fig. 1 shows the schematics of argon inductively coupled plasma (Ar-ICP) device. The ICP torch is composed of coaxial outer and inner tubes. The outer tube has an outer diameter of 18 mm, while the inner tube has

* Corresponding author.

https://doi.org/10.1016/j.tca.2023.179491
Received 14 January 2023; Received in revised form 20 March 2023; Accepted 21 March 2023
Available online 23 March 2023

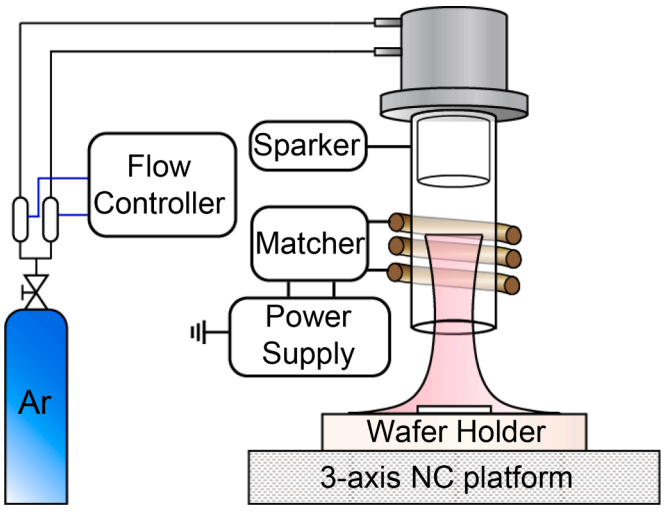

Fig. 1. Schematics of the atmospheric argon inductively coupled plasma (Ar-ICP) setup.

an outer diameter of 16 mm. The thickness of the quartz tube and the gap between the tubes are both 1 mm. The length of the inner and outer tubes are 65 mm and 85 mm, respectively. The cooling gas argon descends through a spiral path between the gap of the tubes to prevent the melting of the quartz tube. Argon is also injected into the inner tube as carrier gas. The flow rate of each gas is controlled by the corresponding mass flow controller. Three turns of coils encircle the outer tube and connect to a radio frequency (RF) power supply. The coil is positioned 2 mm away from the outer diameter of the torch tube, with a diameter of 4 mm. The turns of the coil are spaced 6 mm apart. Circulating cooling water flows through the coils to prevent it from overheating and melting.

The RF power supply provides a high-frequency alternating electric field, which accelerates the free electrons generated by the sparker into high-energy electrons. An impedance matching system is utilized to eliminate the power reflected from the circuit so that the energy is fully coupled to the plasma. The GaN wafer is placed on a piece of quartz holder, the position of which is controlled by a three-axis CNC work stage. The entire ICP equipment is placed inside an enclosure with a ventilation system to prevent possible toxic by-products of the reaction from leaking into the laboratory.

The surface morphology was examined by scanning electron microscope (SEM, Zeiss Merlin). The surface profiles and roughness were measured through scanning white light interferometry (SWLI, Taylor Hobson CCI) and atomic force microscope (AFM, Bruker Dimension Edge). The chemical composition of the GaN surface before and after thermal etching was examined by X-ray photoelectron spectroscopy (XPS, Quantum 2000, ULVAC-PHI) with AlKα radiation (1486.6 eV). All peaks have been calibrated by C1s (284.8 eV) corresponding to carbon contaminations. The species of the plasma were examined by optical emission spectroscopy (OES, Ocean optics USB4000). The GaN surface temperature during thermal etching was measured by an infrared thermal camera (FLIR T660). The weight of the samples was measured by a precision balance (METTLER TOLEDO CC-3372–02). Photoluminescence (PL) spectroscopy measurements at room temperature (300 K) with a helium-cadmium (He-Cd) laser excitation source emitting at 325 nm.

3. Results and discussion

Firstly, thermal etching experiments are conducted in the vacuum furnace to study the process of thermal etching without the influence of argon flow or atmospheric conditions. By focusing solely on the impact of temperature, a more thorough understanding of the thermal etchiOESng process itself can be obtained. GaN is heated under high temperatures in a high-vacuum furnace provided by Thermo Riko co., ltd. An infrared heating device is equipped in the upper part of the setup with a temperature monitoring system adjusting the temperature to the set value. The GaN is placed on a graphite-made sample holder in the quartz chamber. The high vacuum of the chamber is realized through a turbo molecular pump during the thermal etching process. In this experiment, the temperature of the vacuum furnace rises from 25 °C to 1300 °C in 30 s. After that, the temperature is held at 1300 °C for 2 to 10 min. Finally, the infrared heating device is switched off, and the sample cools naturally. The GaN surface morphology after different holding durations of thermal etching is shown in Fig. 2. The majority of the GaN surface remains flat without obvious etching pits after 2 min of thermal etching. After 5 min of holding time, hexagonal-shaped etching pits are formed on the surface. From 5 to 10 min, the edge of hexagonal etching pits gradually becomes irregular, and layered structures can be observed from the edge to the center of the pits. This may be attributed to the emergence of newly-formed small pits along the edge of the pits.

The majority of the GaN surface is relatively flat at the initial stage of thermal etching, as shown in Fig. 2(a). However, some deep etching pits can be observed in certain areas of the surface, as shown in Fig. 3(a). Fig. 3(b) shows the SWLI image and the surface profile a-a' of the areas with deep etching pits. The depth of the etching pits is measured to be around 3 μm. The results indicate that thermal etching preferentially occurs in regions with highly reactive dangling bonds. Fig. 3(c) shows the magnified SEM image of the flat region of the surface. Some nanostructures can be observed on the surface, which indicates that the flat region is also slightly etched. Fig. 3(d) shows the AFM image and the surface profile b-b' of the flat region of the surface. The surface roughness is measured to be *Sa* 0.9 nm, indicating that the surface is still very smooth. The profile b-b' shows that micro etching pits with a depth of 10~15 nm are generated in some areas, which can be considered as the early stage of the deep etching pits.

To further verify the effect of highly reactive dangling bonds on the thermal etching of GaN, scratches were intentionally induced on the surface by a SiC lapping pad. Fig. 4(a) and (b) shows the SEM and SWLI image of the scratched GaN surface, respectively. Many scratches and cracks with abundant dangling bonds have been introduced to the GaN surface. The surface roughness of the scratched surface is *Sa* 14.8 nm. The scratched surface was then thermally etched in a vacuum furnace for 2 min. The majority of the scratched surface is covered by etching pits, as shown in Fig. 4(c). The surface roughness deteriorates to *Sa* 454 nm, as shown in the SWLI image of Fig. 4(d). Compared to the non-scratched sample undergoing the same duration of thermal etching, the scratched surface is more likely to be thermally etched. It is found

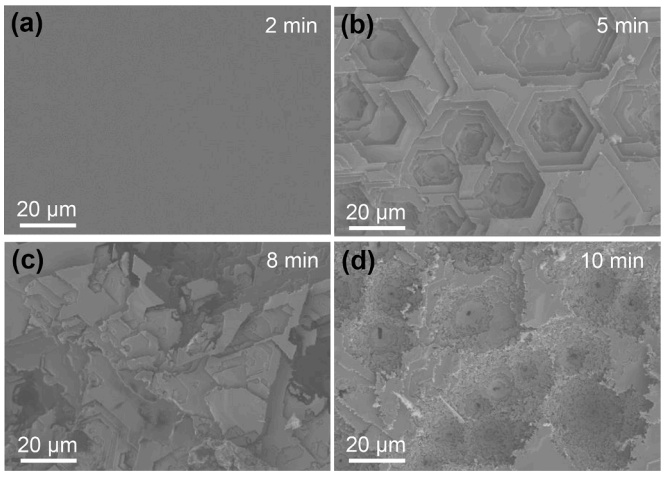

Fig. 2. Surface morphology of GaN thermally etched in a high-vacuum furnace after different holding durations of (a) 2 min; (b) 5 min; (c) 8 min; (d) 10 min.

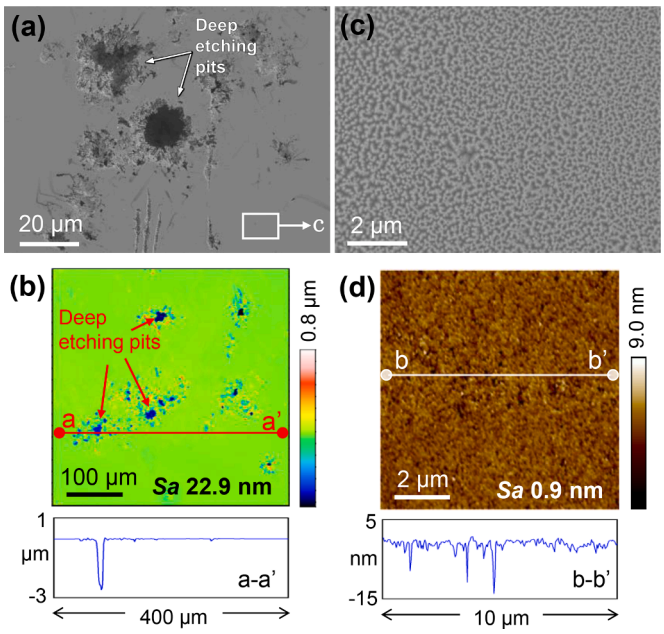

Fig. 3. (a) SEM image of the surface region with deep etching pits. (b) SWLI image and corresponding surface profile of the surface region with deep etching pits. (c) Magnified SEM image of the flat region on the surface. (d) AFM image and corresponding surface profile of the flat region on the surface.

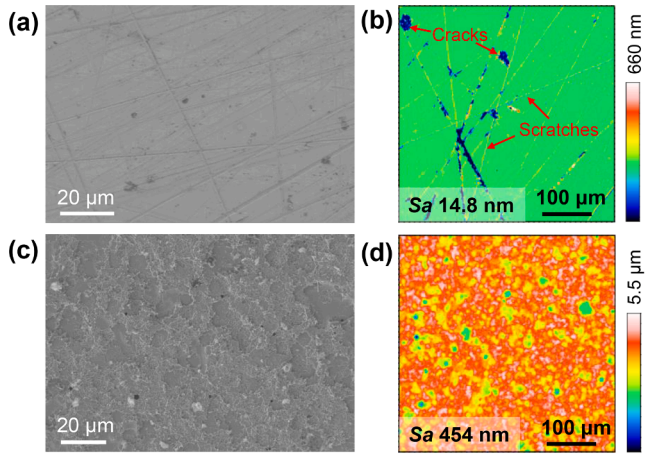

Fig. 4. (a) SEM image of a scratched GaN surface; (b) SWLI image of the GaN surface with cracks and scratches; (c) SEM image of a scratched GaN surface thermally etched for 2 min; (d) SWLI image of a scratched GaN surface thermally etched for 2 min.

that the material removal rate of the non-scratched sample is only 0.6 μm/min. However, the material removal rate of the thermal etching is calculated to be 9.3 μm/min, which is over 10 times higher than that of the non-scratched sample. The above results indicate that the thermal decomposition process of GaN initializes at sites with highly active dangling bonds. Afterwards, deep etching pits are formed on the surface due to the preferential etching along dislocations. The step atoms at the edge of the etching pits also have a higher reaction rate when exposed to the environment, leading to an increase in the dimension of the etching pits.

As a common and easy-to-operate technique, atmospheric inductively coupled plasma can provide high-temperature and high-density plasma and is used as the heat source for the thermal etching of GaN [11]. Inert argon gas acts as a good shield against the external environment, and will not react with the sample as well. This eliminates the requirement for expensive high vacuum maintenance systems and time-consuming vacuuming processes. The working parameters for Ar-ICP thermal etching of GaN are shown in Table. 1.

Fig. 5(a) shows the optical image of the Ar-ICP thermal etching GaN. There is a clear interface where the color of plasma near the surface is purple, while the plasma just ejected from the torch is light pink. The color of the plasma can reflect the existence of excited species in the plasma. The species in the plasma near the sample surface are examined by optical emission spectroscopy (OES). Three sets of experiments were performed to verify the effect of Ar plasma on GaN, as shown in Fig. 5 (b). The OES probe is fixed at a distance of around 150 mm from the center of the ICP torch and is around 1 mm above the sample surface. The integration time of spectra acquisition is 5 ms. The stand-off distance is the length between the torch outlet and the sample surface, which is fixed at 15 mm. For comparison, the spectrum of the Ar plasma is first acquired without GaN placed on the sample stage. The OES spectrum is obtained after the plasma is ignited for 2 min. Meanwhile, very weak N_2^+ peaks located at around 421 nm can be detected, which may originate from the nitrogen in the atmosphere [12,13]. The GaN sample is then placed on the stage with a stand-off distance of 15 mm. Much stronger Ga peaks located at 404 nm and 418 nm can be detected near the surface. Besides, the Ga peaks located at around 288 nm and 295 nm can also be detected [14]. Atmospheric inductively coupled plasma is a kind of fully ionized plasma with a high concentration of ions and radicals. Due to the low mean-free-path of particles, however, ions are unlikely to gain enough energy to break the bonds through sputtering [15]. It can be concluded that Ar inductively coupled plasma can realize the thermal etching of GaN through a decomposition regime. In the thermal etching process, the GaN first decomposes to metallic Ga and N_2, and Ga will be excited to Ga* by high-energy particles in plasma. Finally, the GaN is placed on the stage with a stand-off distance of 25 mm. However, the intensities of these peaks are much lower than that at a stand-off distance of 15 mm. As the stand-off distance increases, the amount of heat transferred to the sample surface decreases, which leads to a lower thermal etching rate. At the same time, the density and energy of particles in the plasma will decrease when they reach the near-surface region, resulting in fewer gallium atoms excited by them. The results show that the larger the stand-off distance, the weaker effect of Ar plasma on the GaN surface. When the stand-off distance exceeds the effective operating length of the plasma at a certain power, the thermal etching effect is not obvious.

To investigate the development of the thermal etching process, OES measurement was also conducted after the plasma was ignited for 20 s, 60 s, and 120 s, respectively. Fig. 5(c) shows the time-resolved OES spectra of the Ar-ICP with a stand-off distance of 15 mm. At a duration of 20 s, a series of obvious Ga-related peaks could be observed. After that, the intensity of Ga-related peaks increases as the duration of thermal etching increases. The higher intensity of Ga-related peaks indicates a higher density of Ga radicals, which also reveals that the thermal etching rate of GaN increases as the duration increases. The detailed material removal rates (MRRs) of Ar-ICP thermal etching measured by weighing methods will be discussed in the following section.

Fig. 6 shows the surface morphology evolution of GaN during thermal etching by Ar-ICP. The RF power is fixed at 600 W, and the stand-off distance is 15 mm. After 10 s of thermal etching, the surface is relatively flat and no obvious etching pits can be observed on the surface. After 30

Table. 1
Working parameters for Ar-ICP thermal etching of GaN.

Parameters	Values
Power frequency	27.12 MHz
Radio-frequency Power	600 W
Gas flow rate	Ar cooling: 18 slm Ar carrier: 1.5 slm
Stand-off distance	15 mm

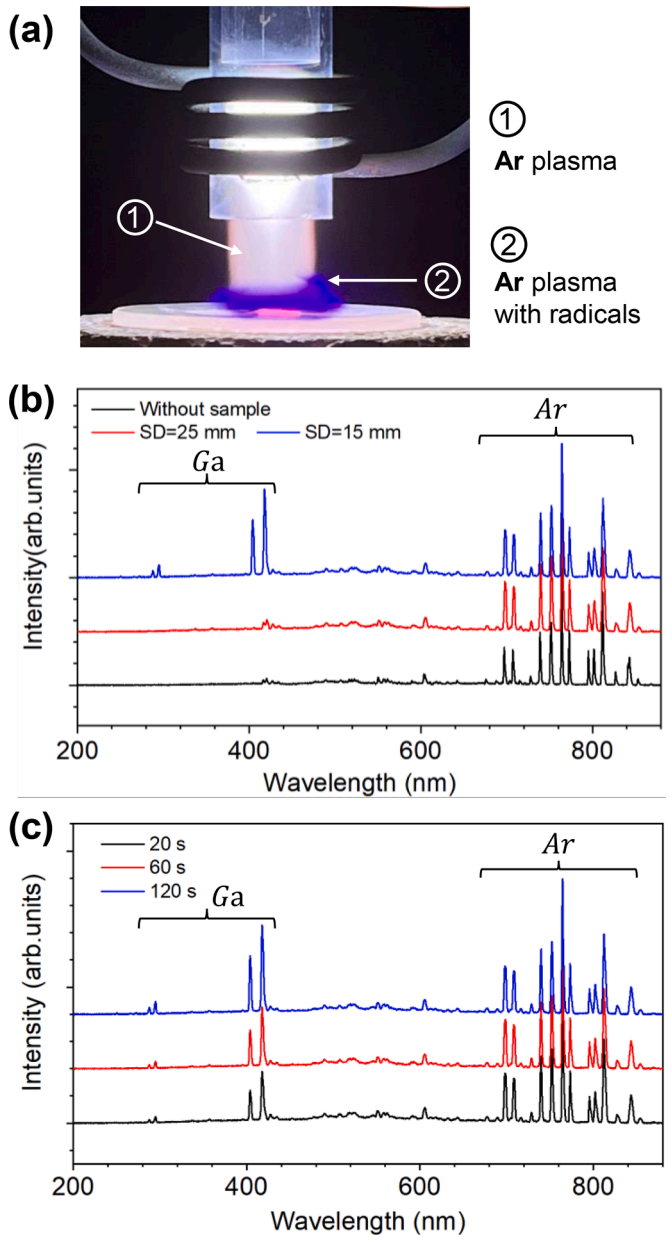

Fig. 5. (a) Optical image of Ar-ICP thermal etching of GaN. (b) Optical emission spectroscopy (OES) of the Ar-ICP obtained near the GaN surface: without sample, SD (stand-off distance)=15 mm, SD=25 mm. (c) OES of the Ar-ICP obtained near the GaN surface after different durations (20 s, 60 s, 120 s).

s, some circular platforms are formed on the surface, which can be attributed to the metallic Ga micro-droplets remaining on the surface. The height of the platform is measured to be around 250 nm, as shown in the AFM image of Fig. 6(c). In the case of the GaN surface after 60 s of etching, circular etching pits with a dimension of around 50 μm can be observed. As the duration of thermal etching further increases to 120 s, the dimension of circular etching pits is enlarged to around 150 μm.

The average temperature of the GaN surface during the Ar-ICP thermal etching is measured by an infrared thermometer. The temperature values of the infrared thermometer are calibrated according to the emissivity of GaN. The temperature variation during the thermal etching is shown in Fig. 7(a). The surface temperature of GaN rises sharply to over 1100 K within 20 s. With the increase of the surface temperature, the heat radiation dissipation increases as well. As a result, the temperature begins to slowly rise to an equilibrium value until the plasma is switched off.

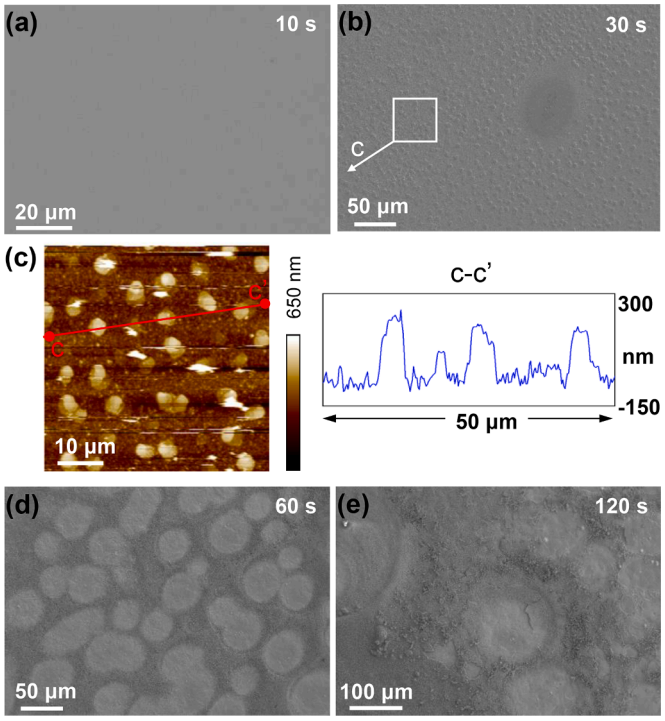

Fig. 6. Surface morphology of GaN after different durations of Ar-ICP thermal etching: (a) SEM image of GaN after 10 s of thermal etching; (b) SEM image of GaN after 30 s of thermal etching; (c) AFM image of micro-droplets formed on the GaN surface after 30 s of thermal etching. (d) SEM image of GaN after 60 s of thermal etching; (e) SEM image of GaN after 120 s of thermal etching.

The MRR is calculated by weighing method, which can be explained by the following equation:

$$\mathrm{MRR} = \frac{\Delta m}{\rho \times S \times t}$$

where Δm is the mass difference, ρ is the density of GaN, S is the surface area, and t is the duration of thermal etching.

The MRRs of Ar-ICP thermal etching under different durations are summarized in Fig. 7(b). In the initial stage, the material removal is relatively small since the temperature is just above the threshold for thermal etching. Only the surface area with highly reactive bonds could be etched. After that, the MRR slowly increases with the increase in duration. The MRR is lower than 0.5 μm/min when the duration is less than 20 s. High temperature is the prerequisite for the thermal etching of GaN, and higher temperature leads to a higher MRR. However, the MRR depends not only on the surface temperature but also on the number of step-edge atoms exposed to the plasma. With the development of the thermal etching process, the etching pit expands and the surface area exposed to the environment increases. From 20 s to 60 s, the MRR begins to increase sharply mainly due to the increase in surface temperature and the number of exposed edge atoms. In the case of etching with a duration of 120 s, the MRR increases to 18.60 μm/min. When the etching duration further increases to 300 s, the MRR does not show a significant change. This is due to the limited increase in surface temperature and surface area exposed to the ambient.

The elemental distribution of the circular etching pits and their surrounding area is measured by energy dispersive X-ray spectroscopy (EDX). Fig. 8(a) shows the GaN surface after 2 min of Ar-ICP thermal etching with circular etching pits. There is more gallium inside the etching pits than in the area surrounding the etching pits, as shown in Fig. 8(b). To further investigate the formation mechanism of the circular etching pits, XPS measurement was conducted for the as-received sample and the sample after 2 min of Ar-ICP thermal etching. The Ga3d

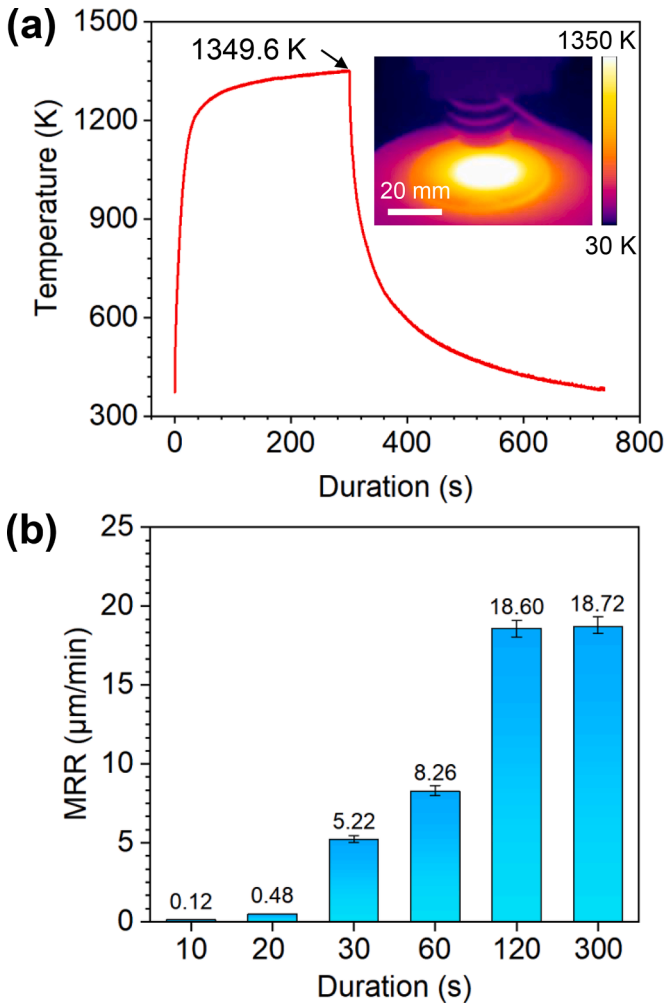

Fig. 7. (a) Temperature variation during the Ar-ICP thermal etching process. (b) Material removal rates of Ar-ICP thermal etching under different durations.

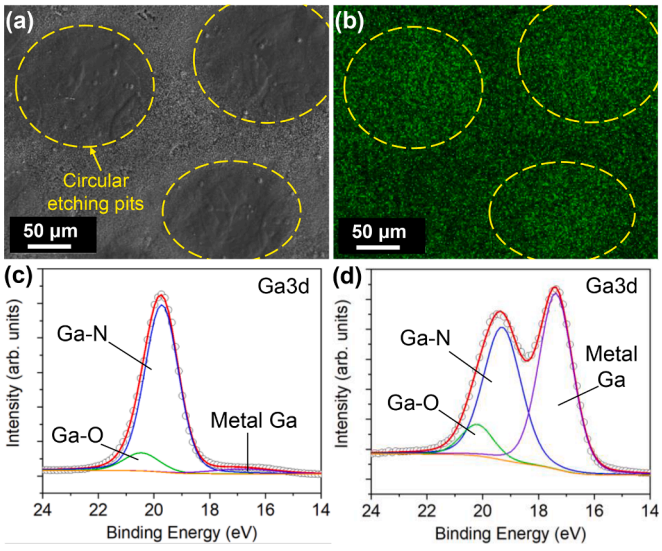

Fig. 8. (a) and (b): (a) Surface morphology and (b) corresponding Ga distribution of the circular etching pits and surrounding regions by EDX mapping. (c) and (d): Core-level XPS spectra of the (c) as-received sample: Ga3d and (d) sample after Ar-ICP etching of 2 min: Ga3d.

spectra of the as-received sample are shown in Fig. 8(c), which can be fitted with three components: Ga-N (19.4 eV), Ga-O (20.3 eV), and metallic Ga (17.3 eV). The results show that the peak intensity of metallic Ga is too low to be detectable. The sample after 2 min of Ar-ICP thermal etching can also be fitted with three components: Ga-N (19.4 eV), Ga-O (20.3 eV), and metallic Ga (17.3 eV). However, the intensity of the peak corresponding to metallic Ga increases to a higher value, as shown in Fig. 8(d), which confirms the generation of metallic Ga on the surface. Combined with the XPS results, it can be inferred that the metallic gallium accumulates in the etching pits. Several probable mechanisms have been proposed for the decomposition of GaN as follows [7,8].

(1) GaN decomposes into liquid gallium and nitrogen:

$$GaN(s) \rightarrow Ga(l) + \frac{1}{2}N_2(g)$$

(2) Sublimation of GaN:

$$GaN(s) \rightarrow GaN(g)$$

The existence of the decomposition regime has been confirmed by the observation of Ga* radicals by OES and the measurement of surface composition by XPS. Based on the above results, the formation mechanism of the circular etching pits during the Ar-ICP thermal etching process is illustrated in Fig. 9. In the initial stage of thermal etching, etching preferentially occurs in some regions with highly reactive dangling bonds and forms micro etching pits, as shown in Fig. 9(a). GaN is first decomposed into metallic Ga and nitrogen, with the nitrogen subsequently detaching from the surface and metallic Ga forming micro-droplets on the surface. After that, these micro-droplets will fill the bottom of the etching pits under the action of argon flow, leading to a relatively low etching rate along the vertical direction. Since the vertical etching is suppressed by the accumulation of metallic Ga, the horizontal etching rate is relatively high and circular etching pits are formed, as shown in Fig. 9(b). Without the action of argon flow, however, it is difficult for the metallic Ga micro-droplets to accumulate at the bottom

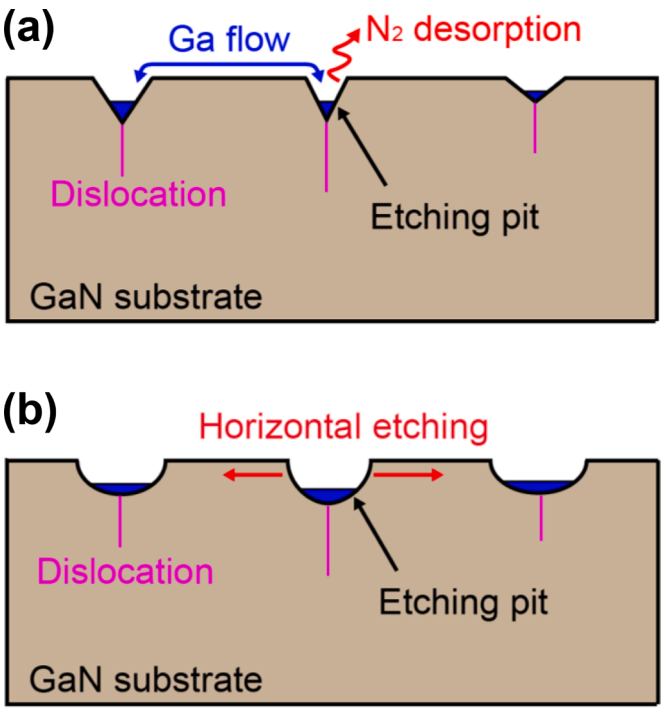

Fig. 9. Schematics of the circular etching pits formation mechanism during the Ar-ICP thermal etching process: (a) Formation of deep etching pits in the initial stage of thermal etching. (b) Metallic Ga accumulates at the bottom of the etching pits.

of the etching pits in the vacuum furnace. Under high temperatures, the metallic Ga micro-droplets will evaporate into gaseous metallic Ga and are pumped out of the chamber. Therefore, the etching pits formed in the vacuum preferentially developed along the vertical direction.

To achieve better performance of GaN-based devices, a smooth surface without subsurface damage and defects is required. The bulk GaN is first sliced into wafers after the crystal growth. After that, the conventional grinding and lapping processes are performed to correct the wafer thickness [16]. However, it is time-consuming for the subsequent polishing processes to remove the damage induced by grinding and lapping [17,18]. The thermal decomposition rate of GaN has been confirmed to be highly efficient in material removal. Hence, it has the potential to achieve highly efficient GaN wafer thinning and damage relief.

The damage relief effect of Ar-ICP etching is also verified by photoluminescence (PL) spectroscopy. The sliced samples are subjected to the Ar-ICP thermal etching and lapping, respectively. A SiC lapping pad with an abrasive size of 70 μm is used for lapping. The RF power of Ar-ICP etching was 600 W, with a stand-off distance of 15 mm. The lapping time and Ar-ICP etching time are both 2 min. Fig. 10 shows the PL spectra of GaN samples after different treatments. In the PL spectra, a near-band emission peaked at 363.1 nm can be observed for the sliced GaN sample [19]. In the case of the sample lapped for 2 min, the peak intensities decrease substantially and the peak position of near-band emission is shifted to 360.1 nm, which could be attributed to the induction of mechanical stress [20,21]. After 2 min of Ar-ICP thermal etching, the peak position of PL spectra shows a redshift to about 363.9 nm, which could be attributed to the damage relief of the GaN sample. In addition, the peak intensity after Ar-ICP etching was about three times higher than that of the sliced sample. However, the intensities of both the Ar-ICP thermally etched sample and the lapped sample are lower than that of the commercial CMP sample. The peak positions of those both show an obvious blue shift compared to the CMP sample as well. The subsurface quality of the sample obtained by Ar-ICP thermal etching is inferior to that of CMP, which may be related to the stress formed during the cooling process.

4. Conclusions

Thermal etching characteristics of GaN have been studied utilizing a high-vacuum furnace and atmospheric argon inductively coupled plasma (Ar-ICP). The following conclusions can be drawn from this study:

1. Hexagonal etching pits are formed during the thermal etching in the high vacuum. Thermal etching preferentially occurs along the surface regions with highly reactive dangling bonds.

2. Thermal etching of GaN can also be achieved by Ar-ICP with a higher etching rate. XPS and OES measurements reveal the thermal decomposition regime of GaN, where GaN is decomposed into metallic gallium and nitrogen during thermal etching.

3. The surface morphology evolution mechanism during thermal etching is investigated. Metallic gallium droplets can be observed in the initial stage of thermal etching. Metallic gallium then accumulates at the bottom of the etching pits under the action of argon flow, leading to the formation of circular etching pits.

4. The photoluminescence intensity of the Ar-ICP thermally etched sample increases and the peak position of near-band emission shows a red shift compared to the lapped sample. Ar-ICP can achieve efficient damage relief compared to the conventional lapping process.

CRediT authorship contribution statement

Linfeng Zhang: Data curation, Methodology, Writing – original draft. **Yongjie Zhang:** Data curation, Methodology. **Bing Wu:** Data curation. **Hui Deng:** Conceptualization, Supervision, Writing – review & editing.

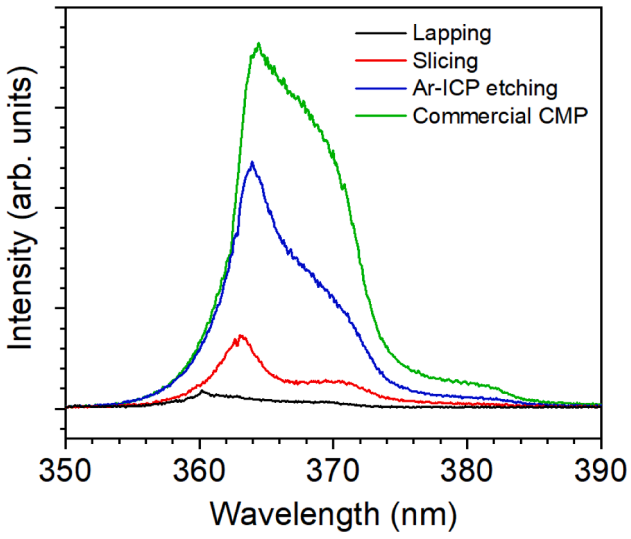

Fig. 10. Photoluminescence spectra of the GaN sample after lapping (black line), slicing (red line), Ar-ICP thermal etching (blue line), and commercial CMP (green line). PL intensity was normalized to an exposure time of 2 ms.

Declaration of Competing Interest

The authors declare that they have no known competing financial interests or personal relationships that could have appeared to influence the work reported in this paper.

Data availability

Data will be made available on request.

Acknowledgments

This project is supported by the National Natural Science Foundation of China (52005243, 52035009) and the Science and Technology Innovation Committee of Shenzhen Municipality (JCYJ20220818100412027, JCYJ20210324120402007). The authors acknowledge the assistance of SUSTech Core Research Facilities.

References

[1] F. Roccaforte, P. Fiorenza, G. Greco, R. Lo Nigro, F. Giannazzo, F. Iucolano, M. Saggio, Emerging trends in wide band gap semiconductors (SiC and GaN) technology for power devices, Microelectron. Eng. 187-188 (2018) 66–77.
[2] Y. Zhong, J. Zhang, S. Wu, L. Jia, X. Yang, Y. Liu, Y. Zhang, Q. Sun, A review on the GaN-on-Si power electronic devices, Fundam. Res. 2 (2022) 462–475.
[3] K. Husna Hamza, D. Nirmal, A review of GaN HEMT broadband power amplifiers, AEU - International Journal of Electronics and Communications 116 (2020), 153040.
[4] K.-.R. Song, D.-.S. Oh, S.-.N. Lee, Optical and crystal improvements of semipolar (11-22) GaN/m-sapphire by in-situ thermal etching process, Curr. Appl Phys. 13 (2013) 1643–1646.
[5] G. Koblmüller, R. Chu, F. Wu, U.K. Mishra, J.S. Speck, Dislocation Reduction in AlGaN/GaN Heterostructures on 4H-SiC by Molecular Beam Epitaxy in the Thermal Decomposition Regime, Appl. Phys. Express 1 (2008), 061103.
[6] P.-.M. Coulon, P. Feng, B. Damilano, S. Vézian, T. Wang, P.A. Shields, Influence of the reactor environment on the selective area thermal etching of GaN nanohole arrays, Sci. Rep. 10 (2020) 5642.
[7] B.V. L'vov, Kinetics and mechanism of thermal decomposition of GaN, Thermochim. Acta 360 (2000) 85–91.
[8] S. Fernández-Garrido, G. Koblmüller, E. Calleja, J.S. Speck, In situ GaN decomposition analysis by quadrupole mass spectrometry and reflection high-energy electron diffraction, J. Appl. Phys. 104 (2008), 033541.
[9] H. Bouazizi, M. Bouzidi, N. Chaaben, Y. El Gmili, J.P. Salvestrini, A. Bchetnia, Observation of the early stages of GaN thermal decomposition at 1200 °C under N 2, Materials Science and Engineering: B 227 (2018) 16–21.
[10] M.E. Lin, B.N. Sverdlov, H. Morkoç, Thermal stability of GaN investigated by low-temperature photoluminescence spectroscopy, Appl. Phys. Lett. 63 (1993) 3625–3627.

[11] C. Tendero, C. Tixier, P. Tristant, J. Desmaison, P. Leprince, Atmospheric pressure plasmas: a review, Spectrochim. Acta Part B 61 (2006) 2–30.
[12] G.Satriyo Wibowo Masruroh, M. Rizky Wijaya, M. Rikza Maulana, D.J.D.H. Santjojo Abdurrouf, Effect of pressure chamber variations on temperature (Te) and electron density (Ne) on nitrogen plasma diagnostics using optical emission spectroscopy, Mater. Today:. Proc. 44 (2021) 3331–3335.
[13] D. Cui, Y. Yin, H. Sun, X. Wang, J. Zhuang, L. Wang, R. Ma, Z. Jiao, Regulation of cellular redox homeostasis in Arabidopsis thaliana seedling by atmospheric pressure cold plasma-generated reactive oxygen/nitrogen species, Ecotoxicol. Environ. Saf. 240 (2022), 113703.
[14] A. Kramida, Ralchenko, Yu., Reader, J. and NIST ASD Team, NIST Atomic Spectra Database(version 5.10), (2022).
[15] L. Bárdos, H. Baránková, Plasma processes at atmospheric and low pressures, Vacuum 83 (2008) 522–527.
[16] H. Aida, 8 - Chemical and physical mechanisms of CMP of gallium nitride, in: S. Babu (Ed.) Advances in Chemical Mechanical Planarization (CMP) (Second Edition), Woodhead Publishing, 2022, pp. 195–221.
[17] H. Aida, H. Takeda, T. Doi, Analysis of mechanically induced subsurface damage and its removal by chemical mechanical polishing for gallium nitride substrate, Precis. Eng. 67 (2021) 350–358.
[18] H. Aida, H. Takeda, S.-.W. Kim, N. Aota, K. Koyama, T. Yamazaki, T. Doi, Evaluation of subsurface damage in GaN substrate induced by mechanical polishing with diamond abrasives, Appl. Surf. Sci. 292 (2014) 531–536.
[19] H. Shin, E. Arkun, D.B. Thomson, P. Miraglia, E. Preble, R. Schlesser, S. Wolter, Z. Sitar, R.F. Davis, Growth and decomposition of bulk GaN: role of the ammonia/nitrogen ratio, J. Cryst. Growth 236 (2002) 529–537.
[20] T.S. Oh, A.H. Park, H. Jeong, H. Kim, T.H. Seo, Y.S. Lee, M.S. Jeong, K.J. Lee, E.-.K. Suh, Spatial stress distribution and optical properties of GaN films grown on convex shape-patterned sapphire substrate by metalorganic chemical vapor deposition, J. Alloys Compd. 509 (2011) 2952–2956.
[21] F. Silie, C. Junfang, G. Peng, W. Chun-ann, Stress analyses of GaN film manufactured by ECR plasma-enhanced chemical vapor deposition, Vacuum 86 (2012) 1517–1521.